IPP-Report

Max-Planck-Institut
für Plasmaphysik

H. Wobig

# Progress in Helias Reactor Studies

IPP III/255

Januar 2000

# Progress in Helias Reactor Studies

T.Amano*, C.D. Beidler, E. Harmeyer, F. Herrnegger, A. Kendl, J. Kisslinger, C. Nührenberg, I. Sidorenko, E. Strumberger, H. Wobig[1]

Max-Planck-Institut für Plasmaphysik, IPP-EURATOM Ass. 85748 Garching bei München, Germany

*National Institute of Fusion Studies, NIFS, Toki, Japan

**Abstract:**

The Helias reactor is an upgraded version of the Wendelstein 7-X experiment, which is under construction in the city of Greifswald. The modular coil system comprises 50 coils, which are constructed using NbTi-superconducting cables. The basic dimensions are: major radius 22 m, average plasma radius 1.8 m, magnetic field on axis 5 T, maximum field on coils 10 T.
Over the past year progress toward better understanding of the fusion plasma has been made. In particular, the following issues have been addressed:

- Plasma equilibrium and MHD-stability
- Neoclassical transport in the Helias configuration
- Start-up scenarios and steady state burn
- Alpha-particle orbits and alpha-particle losses
- Drift waves in Helias configurations
- Modelling the fusion plasma using empirical scaling laws

Technical studies have been focussed on the optimization of the coil system with respect to magnetic field distribution, forces and stresses. In this context the ANSYS-code has been found useful for optimising the support system. In a first survey several blanket concepts, developed for the DEMO tokamak, have been adapted to the Helias geometry. Presently a water-cooled LiPb-blanket is favored in comparison with ceramic breeders, since safety properties and maintenance procedure seem to be more advantageous within this concept. Maintenance and replacement of blanket segments through portholes have also been studied with respect to their geometric compatibility. Finally parameter studies of low aspect ratio Helias reactors will be discussed.

[1] Paper presented at 12th Int. Stellarator Workshop, Madison, Wisconsin, Sept. 29 – Oct. 1, 1999

# 1. Introduction

The Helias (Helical Advanced Stellarator) reactor is an upgraded version of the Wendelstein 7-X device taking into account the design criteria of a power reactor. The magnetic field of this device is a 5 period configuration with some optimized properties. These include reduced Pfirsch-Schlüter currents and the subsequent reduction of the Shafranov shift. The dimensions of a Helias reactor are determined by the following requirements:

- The magnetic configuration is similar to the configuration of Wendelstein 7-X
- There must be sufficient space for blanket and shield
- The magnetic field is small enough to allow for NbTi-superconducting coils
- Plasma confinement must be sufficiently good to provide ignition.
- Thermal fusion power should be about 3000 MW

These requirements have led to the following parameters of the Helias reactor[2].

**Table 1:** Parameters of a Helias reactor

| | | |
|---|---|---|
| Major radius | 22.00 | [m] |
| Minor radius | 1.800 | [m] |
| Plasma volume | 1407 | [$m^3$] |
| Iota(a) | 1.000 | [] |
| Equiv. Current | 3.498 | [MA] |
| Magnetic field on axis | 5 | [T] |
| Max. field on coils | 10.00 | [T] |
| Line average density | 2.126 $10^{20}$ | [$m^{-3}$] |
| Electron density n(0) | 3.040 $10^{20}$ | [$m^{-3}$] |
| Electron temperature T(0) | 15.00 | [keV] |
| Av. electron temperature | 4.965 | [keV] |
| Beta(0) | 15.67 | [%] |
| Average beta | 4.241 | [%] |
| Fusion power | 3000 | [MW] |

These data are obtained by modeling the plasma profiles rather than by solving the transport equations, however the modeling was guided by former results obtained with the ASTRA code[3].
In the following results of Helias reactor studies, which have been obtained recently will be discussed. These encompass further optimization of the vacuum field and subsequent computations of the plasma equilibrium. MHD-stability of these equilibria has been studied using the ballooning mode code JMC and the global mode code CAS3D.
Further physics studies have been concentrated on alpha-particle confinement, neoclassical transport of the thermal plasma and modelling of the start-up phase and the steady state phase of the fusion plasma. Engineering studies have been focussed on the coil system and the optimization of the coil shape in order to reduce the maximum magnetic field in the coils. A further activity has been devoted to a selection of blanket concepts.

[2] C.D. Beidler et al.,IAEA Conf. on Controlled Fusion, IAEA-F1-CN-69/FTP/01, Yokohama 1998
[3] N. Karulin, IPP-report IPP 2/337 (1997)

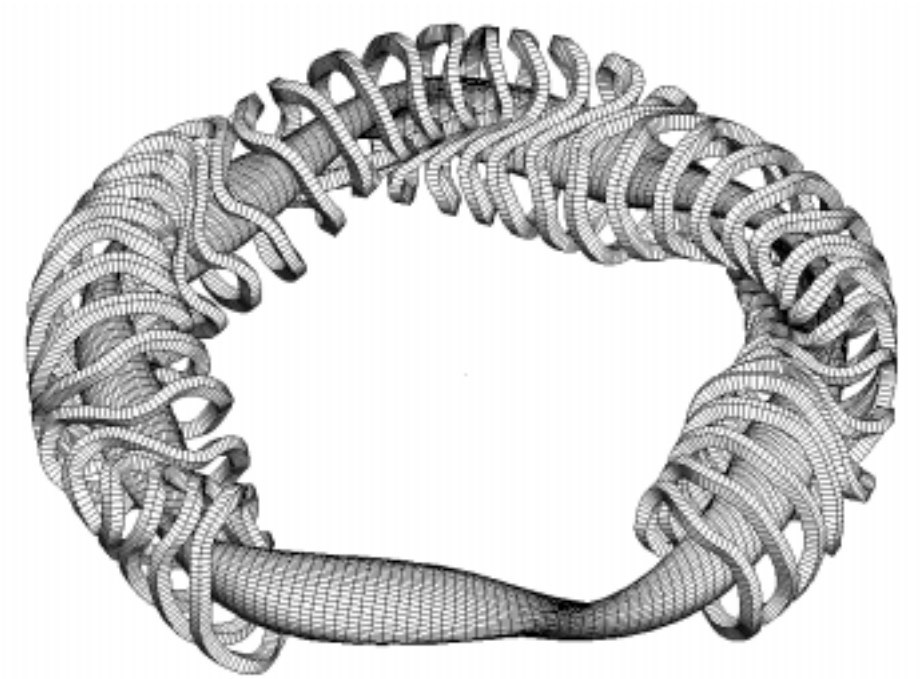

**Fig. 1:** Coil system and magnetic surface of the Helias configuration HSR22

## 1. Plasma equilibrium and stability

The vacuum field of the Helias reactor differs from the standard field of Wendelstein 7-X by a higher toroidal mirror, which is necessary to improve the confinement of the alpha particles. The rotational transform in the plasma center decreases with increasing plasma pressure and low-order rational surfaces, which in the vacuum field do not exist, show up in the finite beta case. In order to avoid the existence of the 5/6 resonance the shear of the vacuum magnetic field has been reduced as much as possible thus avoiding the 5/6 resonance up to a beta value of 4.5%.

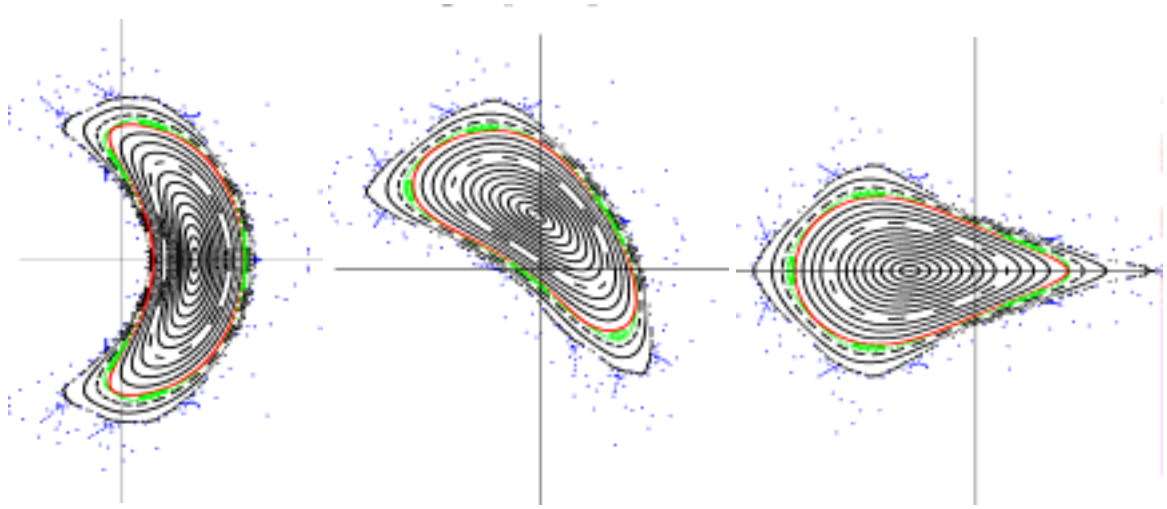

**Fig. 2:** Poincaré plots of the vacuum magnetic surfaces of HSR22

A series of equilibria has been computed using the NEMEC code and the MFBE code[4]. The MFBE code allows one to compute the magnetic field outside the last magnetic sur-

[4] E. Strumberger, C. Nührenberg et al., Proc. 26th EPS-Conf. Maastricht, June 1999

faces, which is the indispensible basis of the divertor design. The magnetic surfaces of the vacuum field are shifted slightly to the inside by an appropriate vertical field, which has been built into the modular coils. The reason is the requirement to center the plasma column in the finite beta state at $<\beta> = 4 - 5\%$ with respect to the first wall. This would lead to equal neutron wall loading at the inboard and the outboard side. Although the plasma equilibrium in the Helias configuration has been optimized, the residual Shafranov shift can grow to 0.5 m.
The structure of the magnetic field and the islands outside the last closed magnetic surface (LCMS) change with rising plasma pressure. The 5 islands at the plasma boundary are envisaged for divertor action and for this reason it is desirable that the structure is nearly invariant to changes of the plasma pressure. In the Helias reactor case the islands grow with plasma beta, however the position of the O-point changes only by a small amount. In view of the envisaged divertor action of the islands this is a very desirable property.

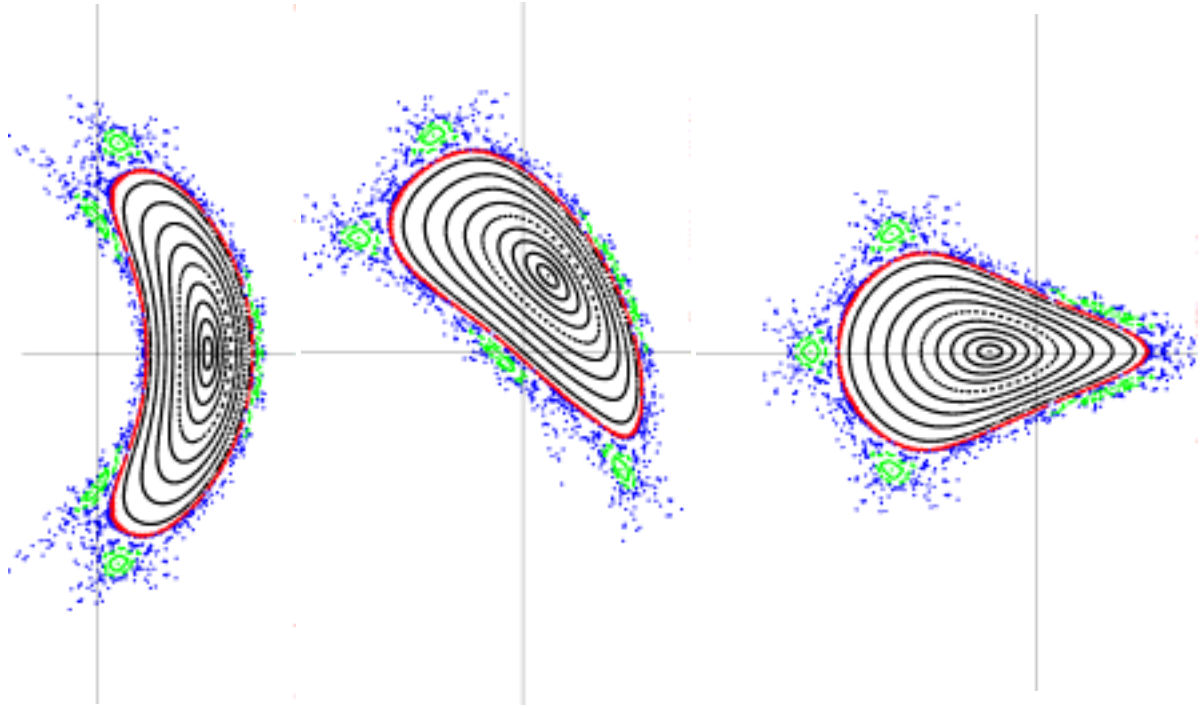

**Fig. 3:** Magnetic surfaces of the Helias reactor HSR22 at $<\beta> = 4\%$

**MHD-stability**

Numerical investigations of the MHD-stability have shown stability up to an averaged beta of 4%. This result was found by local ballooning mode analysis using the JMC-code and by global mode analysis with the CAS3D code[5]. Both methods yield instability at $<\beta>=5\%$. Interpolating the results of CAS3D results in a stability limit of 4.2%[6].
Low order rational magnetic surfaces, which do not exist in the vacuum field, can exist in the finite beta plasma. This concerns the 5/6 resonance, which appears for $<\beta> \geq 4\%$. Since at this point a global mode is expected, the occurance of $\iota(0) = 5/6$ is used as a definition of the MHD-stability limit. The magnetic well deepens with rising beta, which is a decisive feature in providing MHD-stability.

[5] C. Nührenberg, Phys. Fluids **B5** (1993) 3195
[6] E. Strumberger et al., IPP-report IPP III/249

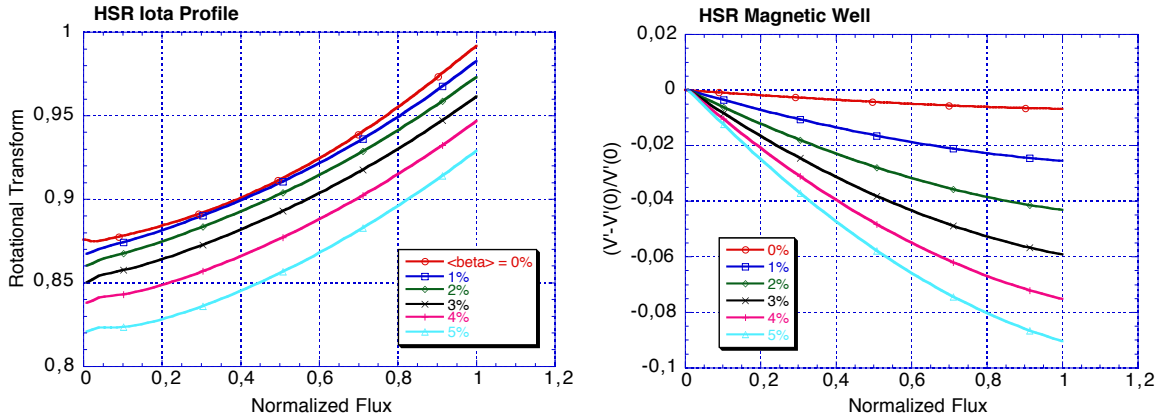


**Fig. 4:** Left Rotational transform at various values of beta. Right: Deepening of magnetic well with rising plasma pressure.

## Drift waves

Drift waves in linear and non-linear approximation have also been studied taking into account the specific geometry of the Helias configuration. In particular, attention has been focussed on the effect of field line curvature and local shear on the linear growth rate of the dissipative drift waves. There is a significant difference between the Wendelstein 7-AS configuration and Wendelstein 7-X, which can be understood mainly by the difference in local shear. The larger local shear in Wendelstein 7-X, which is a by-product of the optimization process, has a stabilising effect on the drift waves[7].

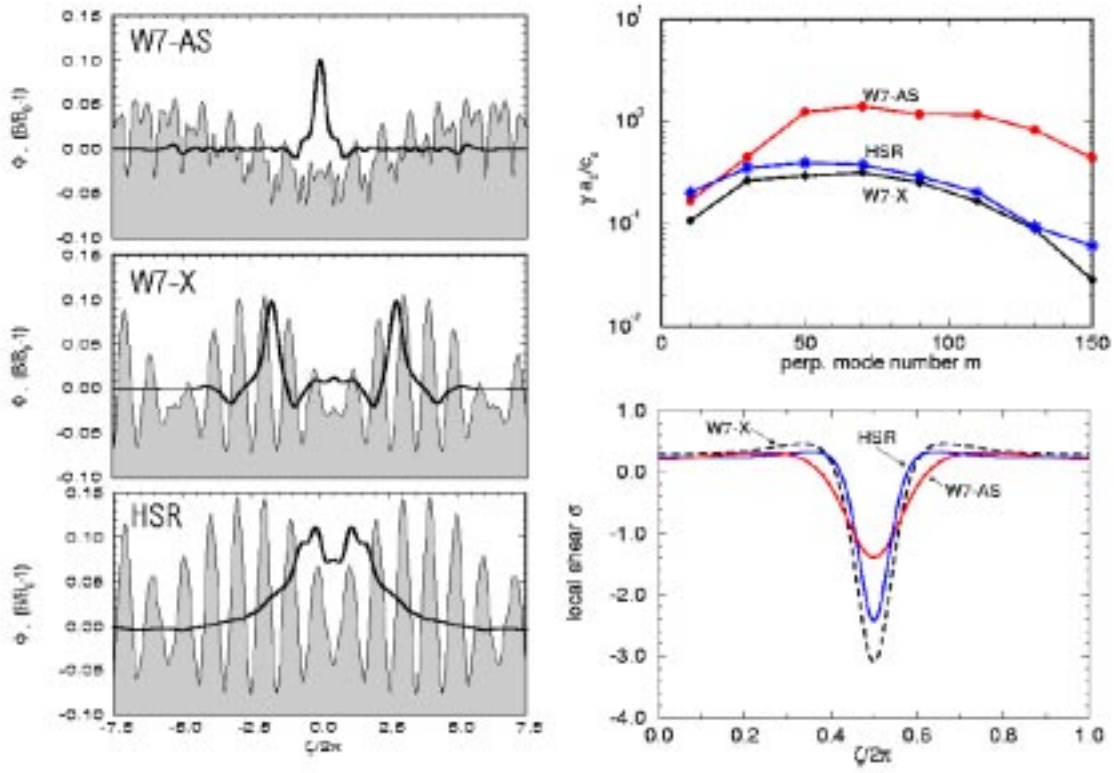


**Fig. 5:** Left: Mode structure of drift wave along field lines. Right: growth rate and local shear in W 7-AS, W 7-X and HSR

[7] A. Kendl, H. Wobig, to be published in *Phys. Plasmas*, see also the paper of Kendl at this conference.

## 2. Neoclassical transport

Computations of neoclassical transport in non-axisymmetric configurations using a Monte-Carlo code or DKES are lengthy and time-consuming. The reason is the complex Fourier spectrum of the magnetic field and the trapping of particles in the various magnetic mirrors of the Helias configuration. For reactor-relevant parameters the ripple-averaged kinetic equation is an appropriate tool to compute these losses. Analytical and numerical approaches to solve this equation [8][9] allow one to compute neoclassical losses on a much faster time scale than any other methods; results for the Helias reactor are presented in the following figures.

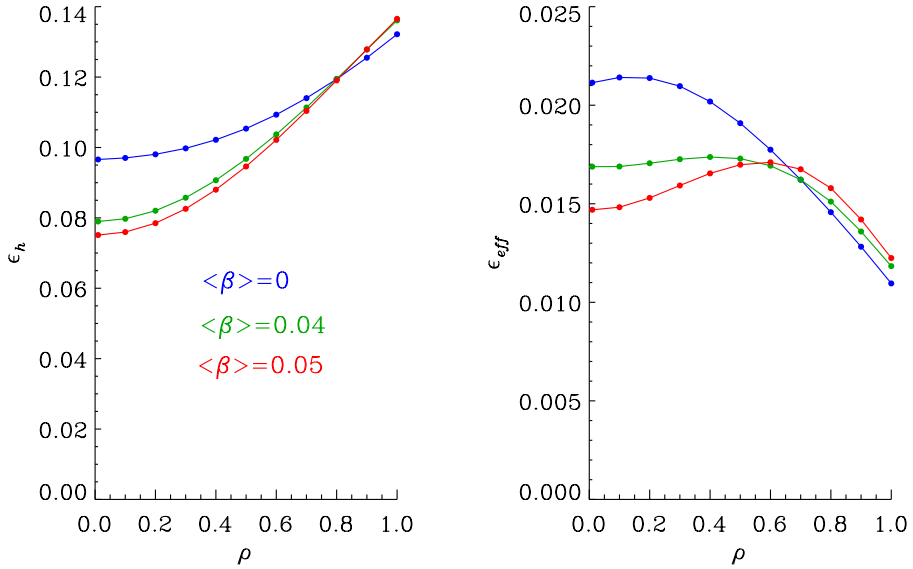


**Fig. 6:** Neoclassical transport in HSR. Geometrical ripple (left) and effective helical ripple (right). Average beta between 0 and 5%.

## 3. Alpha particle confinement

Good confinement of highly energetic alpha particles is a necessary condition for self-sustaining operation of the fusion process in a Helias reactor. In this context the following problems are of importance.

- Sufficient confinement of trapped alpha particles
- A small number of particles traped in the modular ripple
- Anomalous losses of alpha particles by plasma oscillations

Previous investigations (A.V. Zolotukhin) have shown that the losses of alpha particles trapped in a modular ripple can be sufficiently reduced in case of ten modular coils per period. A smaller number of coils would raise the ripple-induced losses appreciably. The majority of trapped alpha particles are trapped in the basic field period. As already shown by W. Lotz et al. poloidal magnetic drift in the finite beta equilibrium improves the confinement of these particles such that only a small fraction of trapped particle is lost in a time shorter than one slowing down time. In the present reactor configuration,

[8] C.D. Beidler, H. Maassberg, IAEA-Technical Committee Meeting, Seeon, Juni 1999
[9] See also the paper by C.D. Beidler at this conference

however, this number is still too large; more than 10% of the heating power is lost by poorly confined alpha particles. Thus, further fine-tuning of the magnetic field is necessary to improve the classical confinement of alpha particles further.
Even after the classical losses of the alpha particles has been minimized to an acceptable level another source of losses may arise due to resonant interaction with electric and magnetic oscillations in the plasma. At the beta limit excitation of Alfvén waves or drift Alfvén waves is to be expected and, if some characteristic frequencies of the particle orbits match the frequencies of the waves, resonant losses may occur. Pfirsch and Wobig[10] have investigated this phenomenon using the mapping technique, which allows one to study the long-term behavior of passing particles. Solving the guiding center equations alpha particle orbits under the influence of time-dependent and time-independent oscillations have also been studied by A.A Shishkin et al[11]. In all these studies the amplitude of the oscillations has been treated as a free parameter, which indicates the need for a self-consistent solution of this issue.

## 4. Ferritic structural material

In stellarators the use of ferromagnetic material has always been a matter of concern, since the vacuum field of the coils may be distorted and the magnetic surfaces may be destroyed. In particular, this issue arises in a Helias reactor where ferritic-martensitic steel is utilized as structural material. Because of its low activation properties this material is highly favored in modern fusion reactor concepts.

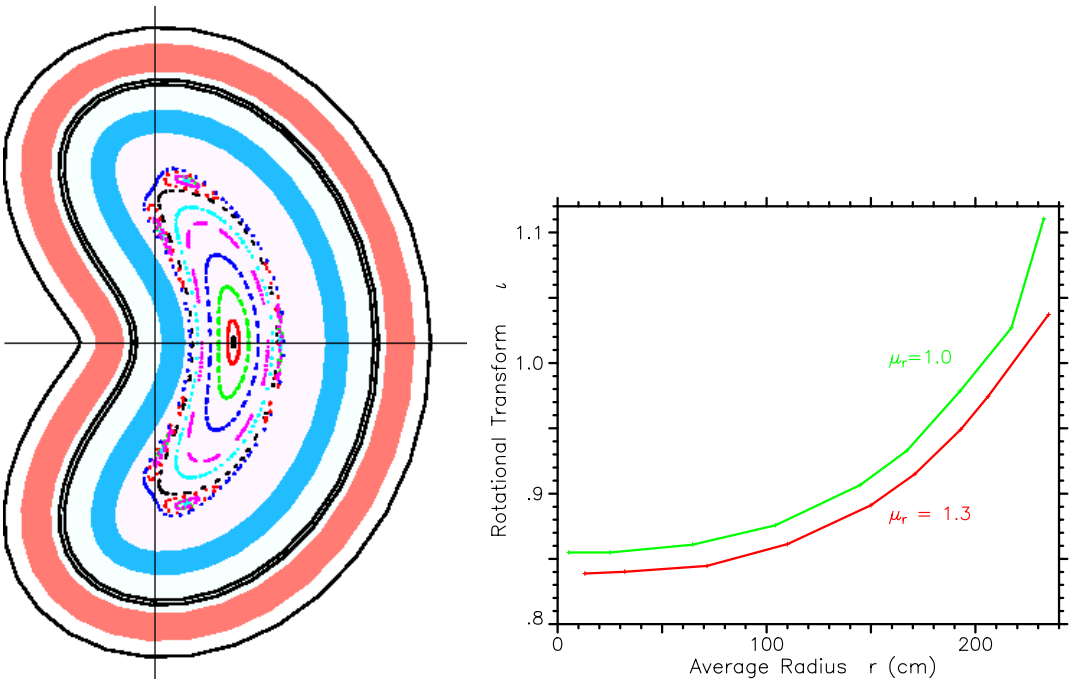


**Fig. 7:** Left: Cross section of the Helias reactor. The plasma is surrounded by a ferromagnetic layer (rel. permeability μ = 1.3, d = 0.4 m, colored blue). The rotational transform is reduced by almost 2% (right side).

The high magnetic field of a fusion reactor drives the steel into saturation and the effective permeability is in the range of 1.3 – 1.5. The distortion of the magnetic field of the

[10] H. Wobig, D. Pfirsch, IPP-report III/245, September 1999
[11] A.A. Shishkin, I. Sidorenko, H. Wobig, IPP Report 2/340, April 1998

coils by ferritic inserts with these properties has been studies analytically in a straight and helically invariant l=2 stellarator and numerically in a Helias reactor[12]. It has been found that the destruction of magnetic surfaces does not occur if the 5-fold symmetry of the configuration is conserved. A small reduction of the rotational transform by 1-2% is not a serious effect and can easily be compensated.

## 5. Island divertor

The rational surface with $\iota = 1$ is located at the plasma boundary. 5 islands exist on this surface which will be used as divertors. The plasma currents tend to modify these islands with rising beta, however it has been found that the position of the O-point is shifted only by a small amount. The increasing ergodization of the surfaces in the island region is not an obstacle to the envisaged divertor action; it may even help to divert the plasma flow. There is a strong similarity to the divertor of a tokamak, except for the helical structure of the X-point. Divertor target plates must follow the helical structure of the X-line. Inherently the structure of the divertor region is three-dimensional and requires a three-dimensional model to describe the plasma behavior in this region. An attempt has been made to approximate the divertor physics by a two-dimensional model by averaging over the coordinate parallel to the X-line. In particular, the heat conduction equation has been reduced to a two-dimensional model, which allows one to study the effect of radiation and the bifurcation phenomena in the divertor region[13].

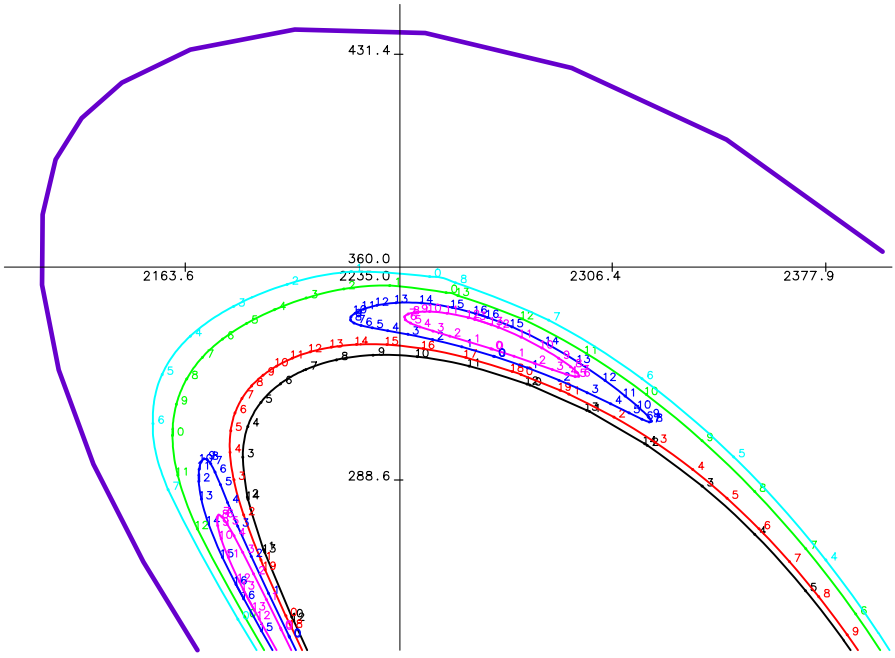


**Fig. 8:** Islands at $\iota = 1.0$ in the HSR vacuum field. The numbers indicate the number of toroidal turns of the field line

[12] E. Harmeyer, J. Kisslinger, H. Wobig, IPP-Report III/241, Mai 1999
[13] D. Sünder, H. Wobig, IPP-Report 2/342, November 1998

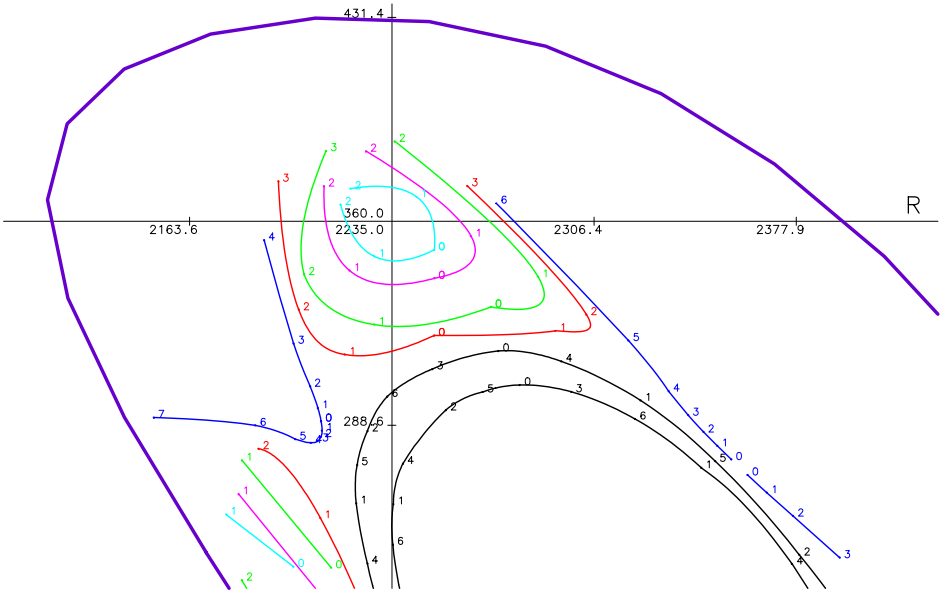


**Fig. 9:** HSR island divertor region. Finite beta plasma at <β> = 4%. Result of VMEC+MFBE.

With the increase of plasma pressure the last magnetic surface shrinks and the islands at ι = 1 grow. The internal rotational transform of the island becomes larger leading to a reduction of the connection length between the plasma side of the island and the back-side of the islands, where the divertor plates will be located. Fig. 9 shows that about three toroidal turns are needed, before the field lines or the flux bundles, which begin close to the separatrix, arrive at the back of the islands. The connection length in this case is about 400 m. The modification of the magnetic structure in the divertor region with growing plasma pressure has some negative effects on the start-up phase or shut-down phase of the discharge, since fixed divertor target plates do not match all magnetic configurations. This issue will be investigated in more detail.
The technical layout of the divertor plates will be very similar to the design in Wendelstein 7-X. The goal is to design the divertor structure as an integrated part of the blanket segments, which certainly will facilitate the maintenance process. The specific power load onto the divertor plates depends on the transport mechanism in the divertor region and the radiative layer. Modeling of these phenomena is being untertaken in close cooperation with the related activities at Wendelstein 7-X and Wendelstein 7-AS.

## 6. Empirical scaling laws and ignition

Modeling fusion plasma with empirical scaling laws has been continued and compared with the results of transport codes. Since stability analysis predicts a beta-limit of 4.2%, the issue arises whether presently known scaling laws of energy confinement are compatible with the requirements of ignition. The ISS95-scaling[14] predicts a confinement time, which is too low by at least a factor of two. Experiments in Wendelstein 7-AS and Wendelstein 7-A are also fitted well by the Lackner-Gottardi scaling, which – if applied to the Helias reactor – meets the ignition condition[15]. This scaling, although it may not

[14] U. Stroth, M. Murakami, R.A. Dory, H. Yamada, S. Okamura, F. Sano, T. Obiki, Nuclear Fusion 36, (1996) 1063
[15] C.D. Beidler, U. Stroth, H. Wobig, Report IPP 2/338, February 1998

be the only one, is also supported by recent experiments in the LHD device. A consistent set of parameters of the fusion plasma is given in the following table.

**Table 2**: Parameters of the fusion plasma

| | | |
|---|---|---|
| Hydrogen Temperature T(0) | 1.500 $10^{01}$ | [keV] |
| Hydrogen Density n(0) | 1.000 $10^{18}$ | [$m^{-3}$] |
| Deuterium Density (0) | 1.300 $10^{20}$ | [$m^{-3}$] |
| Number of Deuterons | 9.444 $10^{22}$ | [ ] |
| Tritium Density n(0) | 1.300 $10^{20}$ | [$m^{-3}$] |
| Number of Tritons | 9.444 $10^{22}$ | [ ] |
| Weight of Tritons | 0.47 | g |
| Impurity Density n(0) | 5.000 $10^{17}$ | [$m^{-3}$] |
| Charge of Impurity | 6 | |
| Helium Density n(0) | 2.000 $10^{19}$ | [$m^{-3}$] |
| Number of 4He Atoms | 1.453 $10^{22}$ | [ ] |
| Alpha Fraction na/ne | 6.579 $10^{00}$ | [%] |
| Beta(0) | 1.567 $10^{01}$ | [% |
| Average Beta | 4.241 $10^{00}$ | [%] |
| Av.Energy Density | 5.711 $10^{-01}$ | [$MJm^{-3}$] |
| Average Temperature | 5.598 $10^{00}$ | [keV] |
| Average Z_eff | 1.181 $10^{00}$ | [ ] |

The peak density in the Helias reactor is assumed to be as high as $3*10^{20}$ $m^{-3}$, which is comparable with the highest densities achieved in Wendelstein 7-AS. This allows one to operate the fusion plasma at low temperature (15 keV), while the fusion output is still sufficiently large.

**Table 3:** Confinement times and fusion power

| | | |
|---|---|---|
| Plasma Energy | 8.036 $10^{02}$ | [MJ] |
| Energy Conf. Time | 1.622 $10^{00}$ | [s] |
| Alpha Conf. Time | 1.337 $10^{01}$ | [s] |
| Energy Conf.Time (LHD) | 5.095 $10^{-01}$ | [s] |
| Energy Conf.Time (LGS) | 1.648 $10^{00}$ | [s] |
| Energy Conf.Time (W7) | 2.092 $10^{00}$ | [s] |
| Energy Conf.Time (ISS) | 9.614 $10^{-01}$ | [s] |
| Bremsstrahlung | 1.003 $10^{02}$ | [MW] |
| Cyclotron Radiation(0) | 1.843 $10^{04}$ | [$W/m^3$] |
| Cyclotron Radiation | 4.264 $10^{00}$ | [MW] |
| Fusion Power | 3.064 $10^{03}$ | [MW] |
| Internal Heating Power | 4.912 $10^{02}$ | [MW] |

Confinement of thermal alpha particles is a matter of concern. If the fraction of thermal alpha particles is greater than 6-7%, the dilution effect leads to an intolerable reduction of the fusion power. A better understanding of the transport losses of thermal alpha particles is necessary.

## 7. Transport code computations

Fusion plasmas in the Helias reactor have also been modeled using the transport code TOTAL_P, which has been developed by T. Amano and K. Yamazaki[16]. In this code all neoclassical transport coefficients including the non-diagonal terms have been retained and, in addition, the radial electric field has been determined by the condition of ambipolarity. The code solves three coupled differential equations of electron temperature, ion temperature and density and computes the time evolution of the profiles. As one of the first results hollow density profiles have been computed, which occur at low density in conjunction with pellet refueling. Hollow density profiles are not very favorable with respect to fusion power output; possibilities how to prevent these profiles need to be studied further.

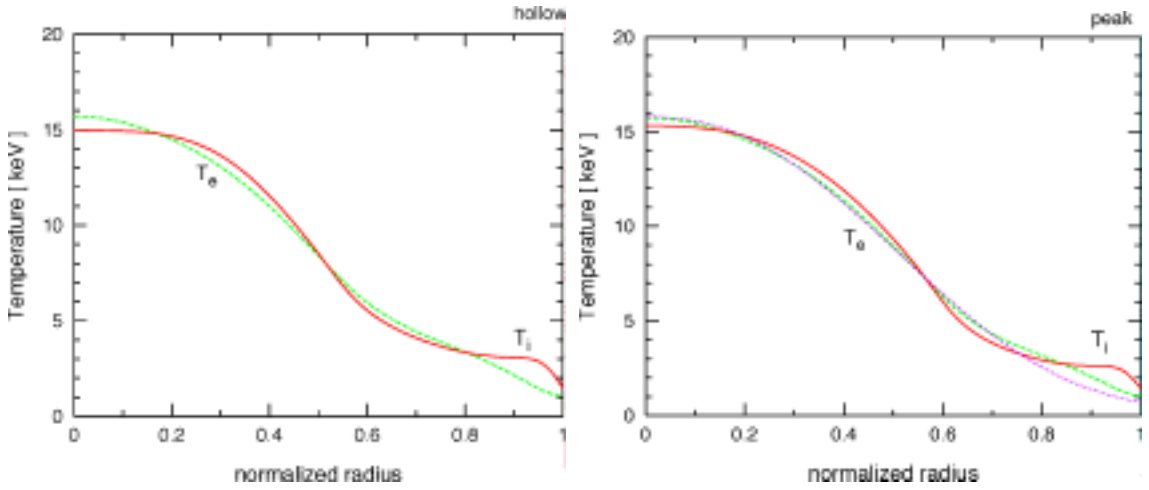


**Fig. 10:** Temperature profiles in HSR, result of TOTAL_P.

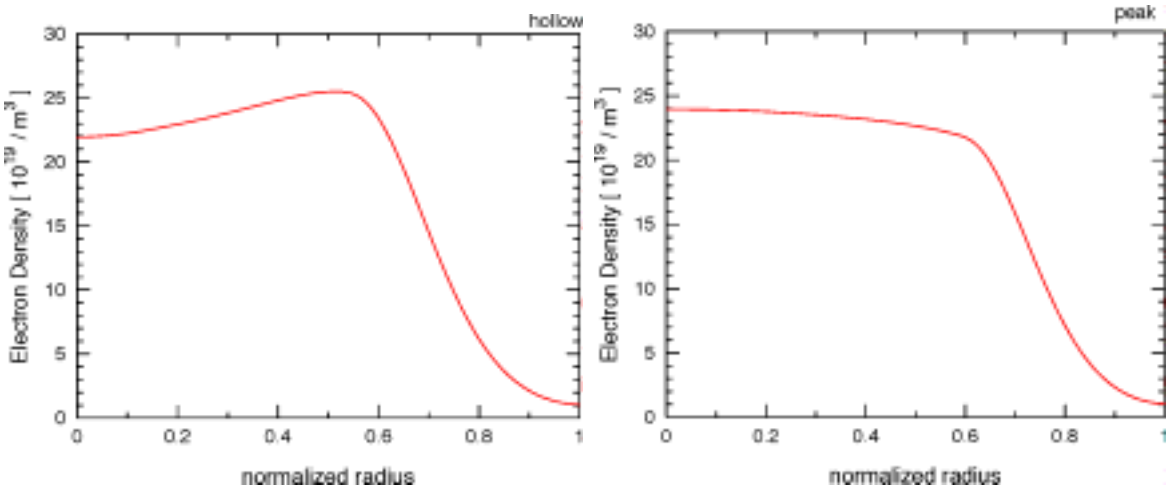


**Fig. 11:** Density profiles in HSR, result of TOTAL_P.

These first results of transport code modeling are in rough agreement with the results of empirical scaling laws.

[16] See also IPP report III/246 Dec. 1999

# 8. Engineering studies

## 8.1. The coil system

The coil system of the Helias reactor consists of 50 modular coils but with only 5 different types. There are 10 coils in every field period and because of the stellarator symmetry only 5 coils have different shapes. Accessibility to the blanket would be facilitated by a smaller number of coils, but this would raise the modular ripple and the losses of highly energetic alpha particles. Concerning the inner structure of the coils large efforts have been made to shape the winding pack in order to reduce the maximum magnetic field in the coils. By shaping the winding pack into a trapezoidal form the maximum magnetic field on the coils could be reduced to 10 T, while the averaged magnetic field on axis is 5 T. There is a sufficient safety margin to the limit of a NbTi-superconductor, if forced flow cooling with super-critical Helium at 1.8 K is applied[17]. In contrast to a former design[18] the windings are wound in double pancakes consisting of 2x18 turns each. The winding process takes place on a winding mould which also seves as a stiffening element of the coils. The dimensions of the superconducting cable are 32x32 mm$^2$.

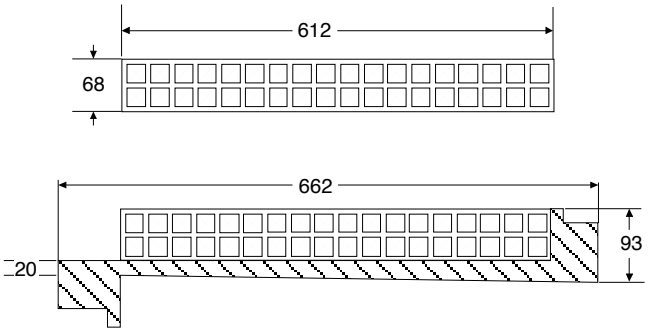


**Fig. 12:** Top: double pancake of the winding pack. Number of turns 2x18. Bottom: double pancake on winding mould.

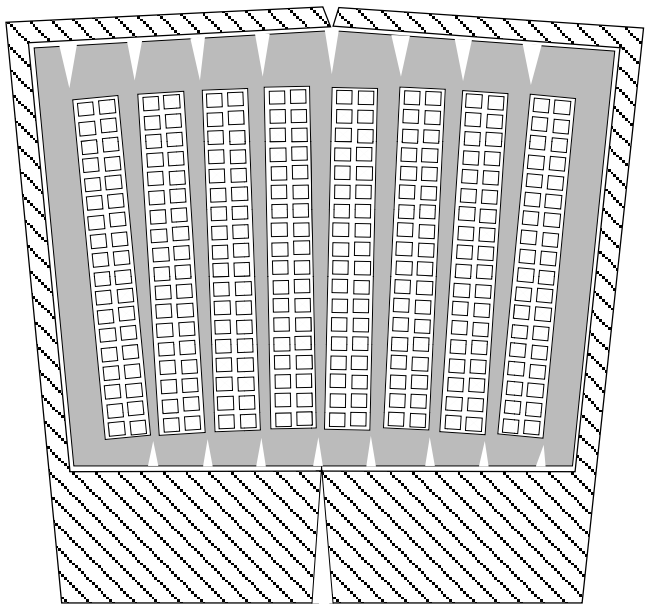

**Fig. 13:** Coil cross-section of the Helias reactor. The inboard side towards the blanket is at the top of the figure.

[17] C.D. Beidler et al. Proc 16th IAEA Conf. on Fusion Energy, Montreal 1996, paper IAEA-Cn-64/G1-4

[18] E. Harmeyer, N. Jaksic, J. Simon Weidner, Proc. 19th SOFT, Lisboa 1996, Vol. II, p. 1035,

The winding is wound onto a winding mould (hatched area in Fig. 12) which also serves as a structural element of the winding pack. 8 of these elements together with the windings are welded together. In contrast to the former concept where the winding pack is wound in layers, the advantage of the pancake technique is that the winding mould is an integrated part of the coil and serves as a stiffening element in the winding pack. The 8 elements are welded together and then enclosed by a coil casing as shown in the next figure (Fig. 13).
Due to the 3-dimensional shape of the coils there are not only radial forces acting on the coils but also lateral forces contribute appreciably to the bending of the coils. The maximum radial force per coil is about 150 MN/m$^3$ and the maximum lateral force is of the same order (120 MN/m$^3$). Integrated forces on the coils stay below 400 MN, however these point in various directions. In the plane $\varphi = 0°$ (center of Fig. 14) the forces point towards the torus center, in the symmetry plane $\varphi = 36°$ (left and right in Fig. 14) these integrated forces are directed in the opposite direction.

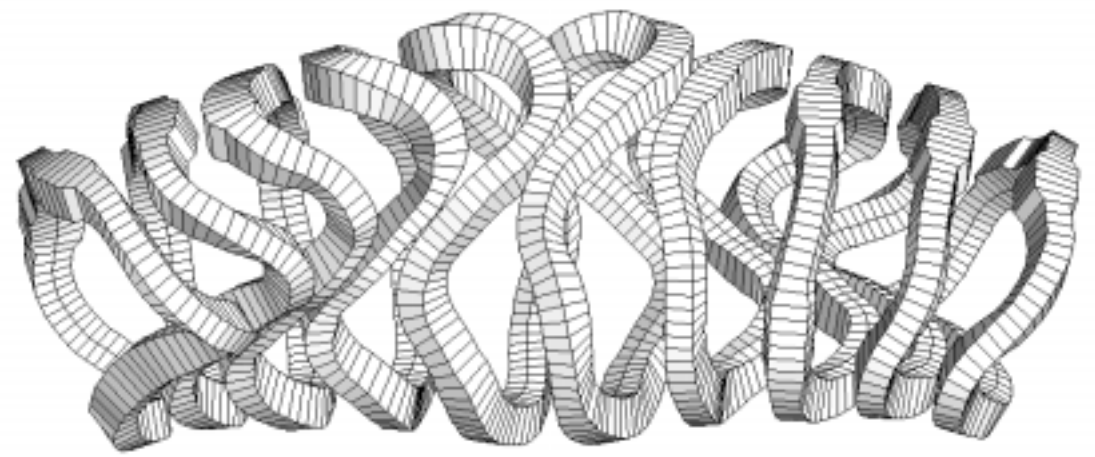

**Fig. 14**: One period of the coil system showing 10 modular coils. The figure displays the coil casing only; intercoil support elements are not shown. Top view onto the coil system.

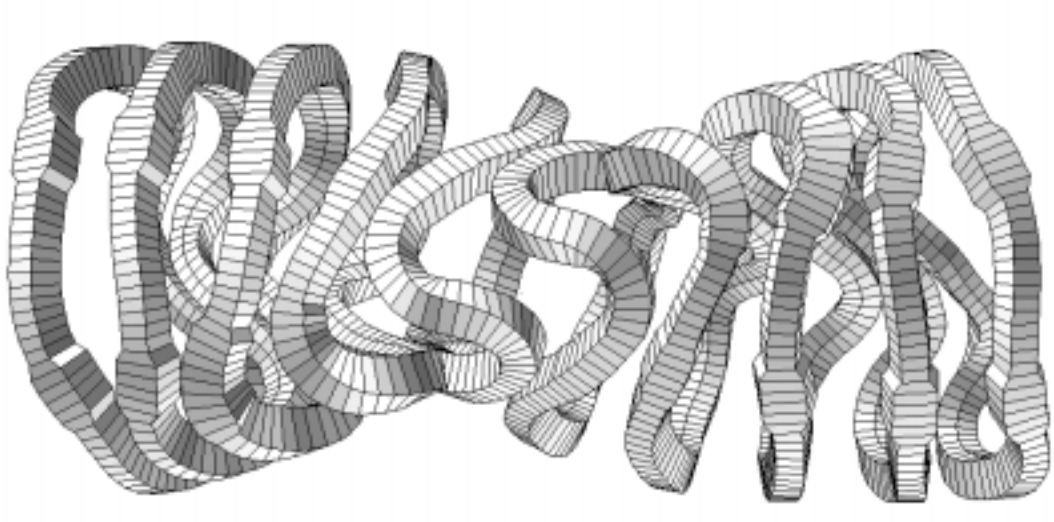

**Fig. 15:** One period of the coil system. View in horizontal direction towards the plasma center.

**Table 4:** Main data of the coil system

| **Helias Reactors** | | **HSB18** | **HSR22-B** |
|---|---|---|---|
| Av. major radius | [m] | 18 | 22 |
| Av. coil radius | [m] | 4.47 | 5.46 |
| Length of cable per coil | [m] | 8981 | 9879 |
| Radial height | [m] | 0.60 | 0.60 |
| Width | [m] | 0.50 | 0.61 |
| Volume of winding pack | [$m^3$] | 8.40 | 12.56 |
| Number of coils | | 50 | 50 |
| Av. specific weight | [$t/m^3$] | 3.39 | 3.39 |
| Mass of winding pack | [t] | 28.49 | 42.56 |
| Total length of NbTi-cable | [m] | 449071 | 493978 |
| Total mass of wdg. pack | [t] | 1369 | 2044 |
| Current density | [$MA/m^2$] | 29.6 | 29.6 |
| Total current | [MA-turns] | 8.85 | 10.82 |
| Casing (height) | [m] | 1.05 | 1.05 |
| Casing (av. width) | [m] | 0.74 | 0.90 |
| Volume | [$m^3$] | 13.30 | 19.86 |
| Specific weight | [$t/m^3$] | 7.90 | 7.90 |
| Mass of Casing | [t] | 105.04 | 156.91 |
| Total Mass of Coils | [t] | 6620 | 9890 |
| Av. Mass of Coil | [t] | 132.41 | 197.80 |
| Support system (volume) | | 438.17 | 800.00 |
| Specific weight | [$t/m^3$] | 7.90 | 7.90 |
| Mass of structure | [t] | 3462 | 6320 |
| Tot. mass of coil system | [t] | 10082 | 16210 |
| Field on axis | [T] | 5 | 5 |
| Max. field on coils | [T] | 10 | 10.07 |
| Magnetic energy | [GJ] | 54 | 99 |

The first column (HSB18) describes the data of a Helias ignition experiment, where the blanket has been reduced as much as possible and the breeding of tritium has been dropped. The rationale is that of the ITER-experiment, where the blanket only serves as protection for the coils. Ignition in this reduced configuration is a critical issue since the Lackner-Gottardi scaling predicts a confinement time, which is too small. Only if the Wendelstein-scaling holds is the projected confinement time large enough for ignition.

**Stress calculations**

Stresses in the coils depend strongly on the geometry of the support system. This support system consists of the coil casing and the intercoil support elements. In designing this support system a compromise could be reached between the need to minimize the stresses and the desire for optimum access to blanket and the plasma chamber. Stress analysis is performed using the ANSYS code[19]. Orthotropic elastic data of the proposed cable in conduit conductor are used for these computations as approximation to the complex winding pack, which consists of superconducting strands, copper, aluminum alloy and insulating material. The elastic data of the coil casing and the support elements are those of stainless steel, the elastic data of the winding pack are those of Wendelstein 7-X.

[19] O. Jandl, E. Harmeyer, Proc. of 15th Int. Conf. on COMP. MECHANICS. 99, Nectiny, CZ, 133 - 140

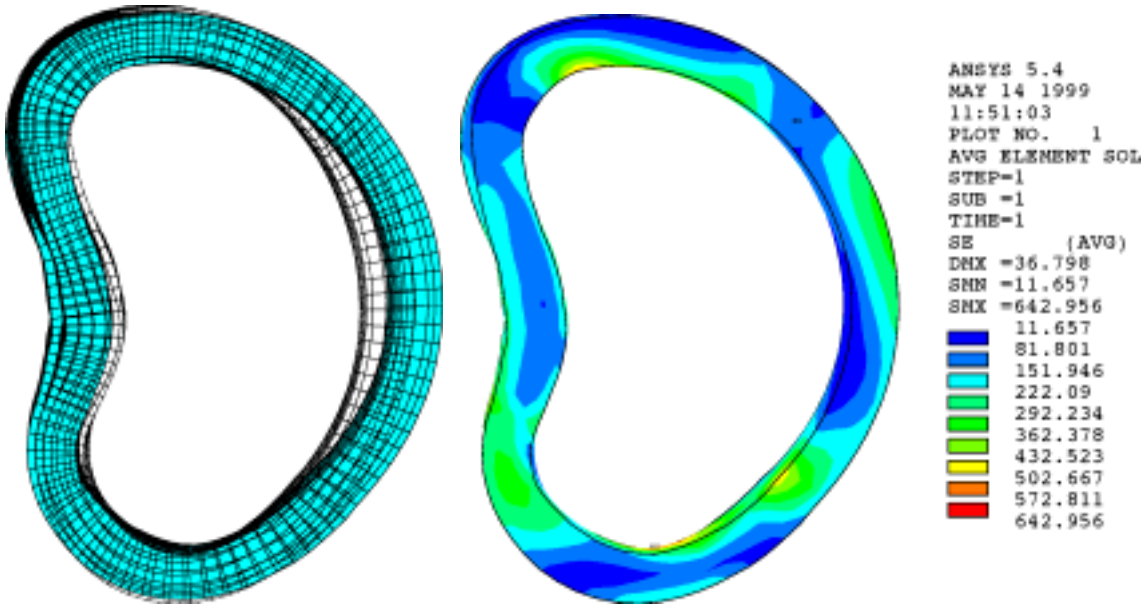


**Fig. 16:** Left: Displacement of coil1, maximum displacement 37 mm. Right: van Mises stress in the coil casing, peak value 542 Mpa. Forces of coil1 only.

**Intercoil support system**

The intercoil support structure is modeled similarly to earlier studies (Ref. 17), but care has been taken to provide sufficient space for the maintenance procedure. The coil winding pack is embedded in the coil casing separated by epoxy in between. Non-linear contact elements are applied in the ANSYS code, which only transfer compression forces. The maximum stress found in the coil housing is 650 MPa. Locally the deformation is larger than 0.2%, which implies that further optimization of the support system is needed to reduce the local stress maxima.

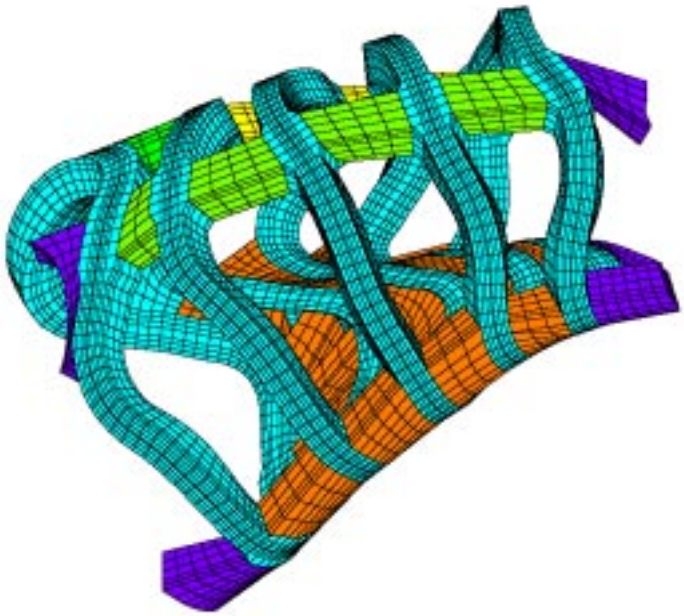

**Fig. 17:** 5 modular coils in a field period and the intercoil support elements

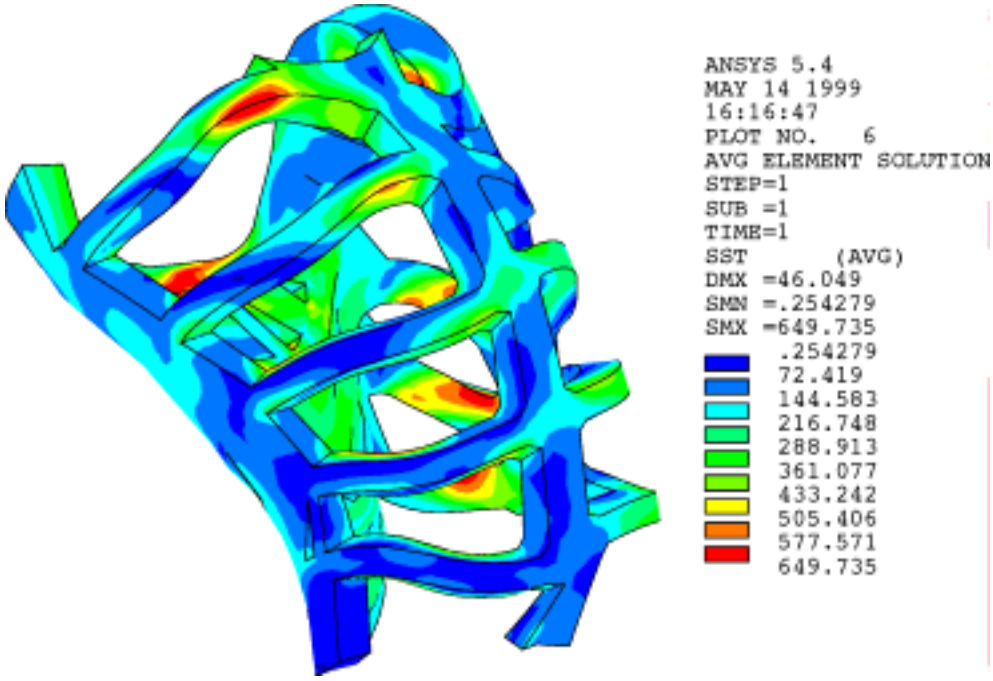


**Fig. 18:** Stresses in the coil support system and the coil casings. Maximum van Mises stress 650 Mpa.

**Stresses in winding pack**

First results of the stress in the winding pack are shown in the following figure. In the superconducting windings the stresses are not higher than 40 Mpa.

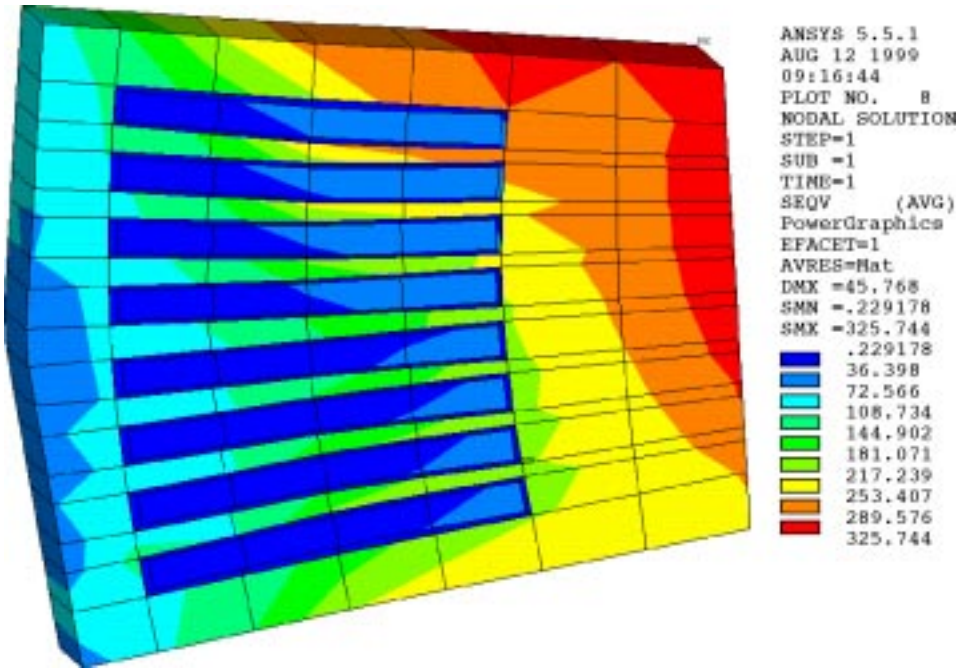


**Fig. 19:** van Mises stress in the coil winding pack. Max. stress 325 Mpa.

The stresses shown in Fig. 19 are computed with the forces of coil one only.

## 8.2. Blanket design in the Helias reactor HSR22

The dimensions of the Helias reactor are mainly determined by the need to accomodate a breeding blanket and a shield. In the narrowest region on the inboard side the distance between plasma surface and coil casing is 1.5 m, which leaves a gap of 1.3 m for blanket and shield. In other places around the torus the gap is wider, it can reach nearly 2 m. In the frame of the NET-ITER activity several blanket concepts have been developed and one of the goals in Helias reactor studies was to transfer these concepts to the Helias reactor and to make a critical assessment of the advantages and disadvantages of the various concepts[20].
The options in the Helias reactor are:

- Helium-cooled solid breeder blanket (HCPB)
- Helium cooled Li-Pb blanket
- Water-cooled Li-Pb blanket (WCLL)

Two major differences between a tokamak reactor and a Helias reactor are decisive with respect to blanket design; these are the three-dimensional shape of the blanket and the large area of the first wall. In the present concept this area is 2600 $m^2$ which leads to an averaged neutron wall loading of less than 1 $MW/m^2$ (fusion power 3000 MW). The peak wall loading is 1.7 $MW/m^2$. As the result the lifetime of first wall and plasma facing components is larger than in a compact tokamak reactor. Compared with the DEMO tokamak reactor, where a lifetime of 2.3 years[21] (70 dpa in the structural material) is assumed, the lifetime of plasma facing components and blanket elements would be about 4.6 years. Since in present material studies a limit of 140 dpa is considered as realistic, the lifetime of components in the Helias reactor may reach 9 years.

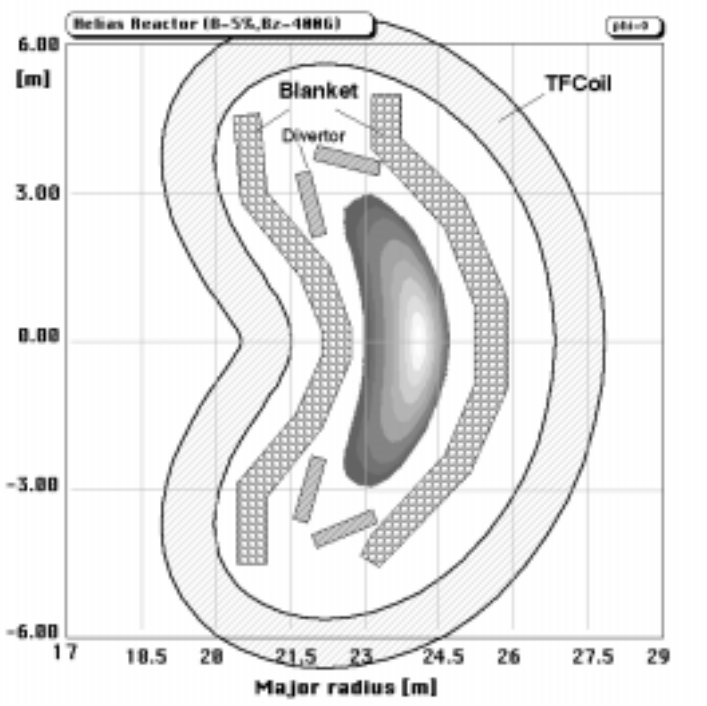


**Fig. 20:** Scheme of breeding blanket modules in the φ=0° plane. The plasma beta is 5%. Also the divertor target plates are displayed schematically.

[20] H. Wobig, E. Harmeyer, F. Herrnegger, J. Kisslinger, IPP-report III/244
[21] M. Dalle-Donne et al. KfK Report KfK 5429, Nov. 1994

Various aspects determine the choice of the blanket: geometrical complexity, tritium inventory, MHD losses, maintenance and recycling procedure. Although the magnetic field in a Helias reactor is slightly smaller the MHD losses in the Li-Pb eutectic are too large to install the self-cooled or helium cooled Li-Pb blanket. Because of the large amount of beryllium needed in the solid breeder blanket and the accumulated tritium inventory in the beryllium there are some arguments against this concept. On the other hand swelling of beryllium, which is believed to be a limiting property in the HCPB concept, can be reduced in the Helias reactor due to the lower temperature in the blanket. The reason for the reduced temperature in the blanket is the factor two smaller power deposition per volume element as compared to the tokamak reactor. After replacement the blanket elements of the HCPB concept must by reprocessed in order to recover the beryllium and to extract the accumulated tritium. This will certainly be a cost-driving factor of the blanket.

**Table 5:** Parameters of the solid breeder blanket in HSR22

| | |
|---|---|
| Neutron wall loading | 0.92 $MWm^{-2}$ |
| Peaking factor (inboard/outboard) | 1.7 |
| Maximum surface heat flux | 0.4 $MWm^{-2}$ |
| Coolant Helium | |
| Temperature (inlet/outlet) | 250/450 °C |
| Average pressure | 8 MPa |
| Breeding Zone | |
| Breeder $Li_4SiO_4$, Multiplier Be pebbles | |
| Number of segments (inboard /outboard) | 250 |
| Length (inboard /outboard) | 10 m |
| Total mass of breeder | 201 tons |
| Total mass of Beryllium | 843 tons |
| Mass of structure | 1907 tons |
| Total mass of breeder zone | 2951 tons |
| Weight per segment | 10.5 tons |
| Shield/Manifolds | |
| Total mass | 4131 tons |
| Total (blanket/shield) | 7082 tons |
| Lifetime (70 dpa) | 47800 hours (5.5 y) |

The water-cooled Li-Pb blanket is the present candidate as the breeding blanket in the Helias reactor. Tritium and other activated material can be permanently extracted from the liquid breeder and after shutdown of the power plant the breeder material is reusable. The blanket segments consist of the structural walls and cooling pipes and the liquid breeder can be stored in separate tanks during the replacement procedure. To prepare the activated blanket segments for permanent waste disposal, a complicated reproccessing cycle is not necessary. A disadvantage is the weight of the liquid breeder material, which requires the corresponding support elements of the vaccum tube. Thermal efficiency of the power conversion cycle is rather moderate, since water is used as a coolant the temperature in the thermal cycle stays below 350° C and the efficiency of the conversion to electricity is on the order of 35%. Some recycling power will be needed for the cryogenic system and the pumping system, which will reduce the overall efficiency of the plant by some percent.

**Table 6:** Parameters of the liquid breeder blanket in HSR22

| | |
|---|---|
| Av. neutron wall loading | 0.92 $MWm^{-2}$ |
| Peaking factor | 1.7 |
| Maximum thermal load on first wall | 0.23 $MWm^{-2}$ |
| Av. length of segment | 10 m |
| Volume of segment | 8 $m^3$ |
| Weight of segment | 55.6 tons |
| Weight of Pb-Li per segment | 44.7 tons |
| Weight of structure | 6.9 tons |
| Number of segments | 280 |
| Breeder Pb-17Li | |
| Inlet/outlet temperature | 260/325° C |
| Average velocity | 5 mm/s |
| Coolant $H_2O$ | |
| Pressure | 15.5 Mpa |
| Inlet/outlet temperature | 260/325° C |
| Maximum velocity | ? |
| Av. nuclear power in segment | 8.6 MW |
| Number of different shapes | 25 |
| Total weight (with breeder) | 14450 tons |
| Weight of Pb-17Li | 12525 tons |
| Weight of structure | 1920 tons |
| Volume of segments | 2240 $m^3$ |
| Lifetime (70 dpa) | 47800 hours (5.5 y) |

## 8.3. Maintenance

In contrast to earlier concepts of maintenance and repair, in which a whole period of the coil system is horizontally withdrawn, it is now proposed to replace blanket segments through portholes between the coils. In every period there are 8 big portholes available, 4 on the top and 4 at the bottom of the period (see Fig. 14). Typical dimensions of the port-holes are 2x6 $m^2$. Also in the horizontal direction large portholes are available as can be seen in Fig. 15. The number of segments in HSR22 is 250; in one field period there are 50 blanket segments. Because of the symmetry of the stellarator configuration there are only 25 segments with different shapes. The size of one segment is roughly 1x1x10 $m^3$ and it has been studied how these blanket segments can be installed through the port-holes. The two blanket concepts presented in the previous chapter differ with respect to their maintenance procedure. While the segments of the solid breeder blanket must be installed and removed fully equipped with breeder material and neutron multiplier, the segments of the LiPb-concepts can be replaced without the liquid breeder material.

Divertor target plates are another component, which need replacement after their life-time. This issue is presently under investigation and the aim is to design the target plates as an integrated part of the blanket segments where replacement of blanket and target plates happens simultaneously.

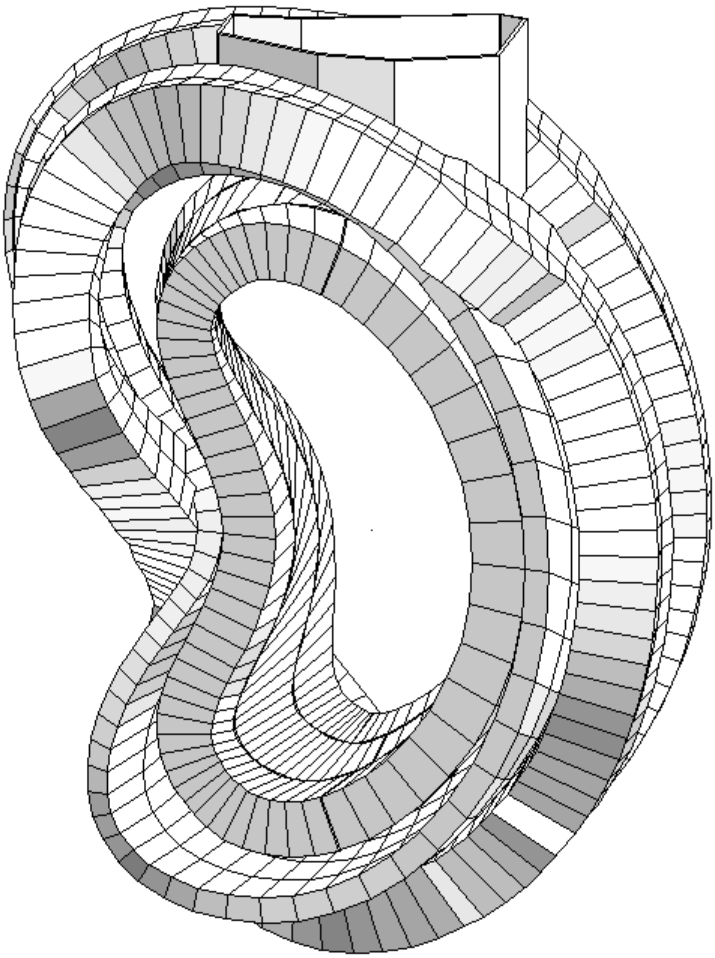

**Fig. 21**: Coils in plane $\varphi = 0°$, shield and blanket modules. The replacement of the 6 blanket segments can be made through the porthole at the top. Blanket segments are fixed to the vacuum tube, which also serves as shield for the coils.

## 9. Alternative concepts

Parameter studies have begun to explore alternatives to the 5-period Helias configuration[22]. The goal is to reduce the aspect ratio and to achieve a more compact device[23]. Alternatives are 4 periods and 3 periods, which can be modeled by starting from the 5-period HSR22 (R = 22 m) and by removing one or two periods while the space for blanket and shield is kept fixed. The next table summarizes the main parameters of some of these alternatives.

[22] J. Kisslinger, C.D. Beidler, E. Strumberger, H. Wobig, *Low aspect ratio Helias configurations*, see paper at this conference.

[23] Quasi-omnigeneous stellarators (QOS) are examples of compact devices (see D.A. Spong et al., IAEA-F1-CN69/ICP 07, Proc. 17th IAEA Conf., Yokohama 1998). Another example is the quasi-axisymmetric stellarator (QAS) (A. Reiman et al., IAEA-F1-CN69/ICP 06, Proc. 17th IAEA Conf., Yokohama 1998 )

**Table 7**: Paremeters of reduced aspect ratio Helias reactors

| Periods | R [m] | a [m] | A = R/a | ι(0) | ι(a) | δV'/V' [%] |
|---|---|---|---|---|---|---|
| 5 | 22 | 2.05 | 10.7 | 0.87 | 5/5 | -0.7 |
| 4 | 18 | 2.10 | 8.5 | 0.69 | 4/5 | -1 |
| 4 | 18 | 2.12 | 8.5 | 0.83 | 4/4 | -2.5 |
| 3 | 15 | 2.26 | 6.6 | 0.63 | 3/4 | -4 |

The first line decribes the low shear standard configuration HSR22. The second and the third are 4-period configurations; the second one has nearly the same iota profile as the standard case HSR22. Plasma aspect ratio can be reduced to 6.6 in the 3-period configuration.

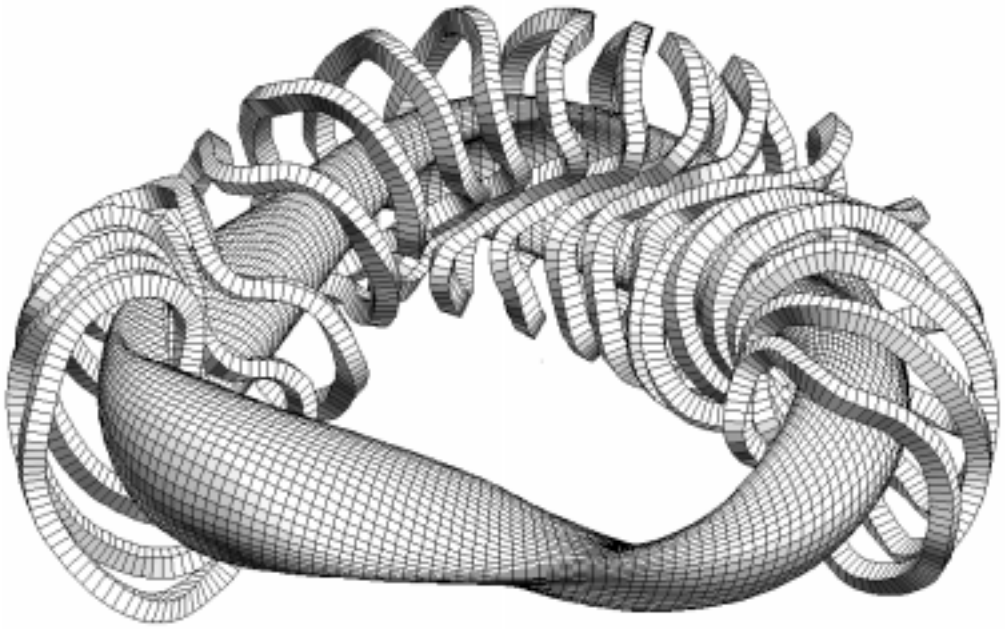

**Fig. 22:** 3-period Helias configuration.

One disadvantage of the low aspect ratio configurations is a larger ratio of the magnetic field on the coils to the average field on the magnetic axis, which leads to an increase of the electromagnetic forces on the coils. Since in NbTi superconductors the field strength on the coils is a limiting value, a reduction of the field strength in the plasma region is unavoidable. If this for reasons of confinement is not tolerable, the use of NbSn superconductors must be considered. Another problem arises in compact devices if the fusion power is kept constant at 3000 MW. The specific neutron wall load will increase to more than 1 MW/m$^2$ and as a consequence the lifetime of the first wall will decrease.

## 10. Conclusions

Significant progress has been achieved in understanding the physics issues of a Helias fusion reactor. This refers to a clearer picture of the plasma equilibrium and the plasma stability. There is a chance to run the Helias reactor in stable operation at $\langle\beta\rangle = 4.2\%$ and to deliver a fusion power output of 3000 MW. Projections of present-day empirical scaling laws are not in contradiction to the requirement of a self-sustained fusion discharge; first results of the LHD experiment justify some optimism that these scaling laws can be extrapolated to the reactor regime. Dilution of the fusion plasma by thermal

alpha particles is still an issue. It is closely related to the neoclassical accumulation of impurity ions in the plasma center. However, it is expected that the fusion plasma stays at the beta limit, where the onset of MHD-instability leads to increased plasma losses and thus stabilizes the thermal instability. Transport of all ion species will be anomalous under these circumstances and it is hard to say whether the neoclassical predictions will apply.

The divertor concept in the Helias reactor relies upon on the efficacy of the island divertor. This island divertor will be installed and tested in the Wendelstein 7-X device and it is designed for a power load of 10 MW/m$^2$. If this is achievable under reactor conditions a wetted area of about 40 m$^2$ would be needed in HSR

Because of the large area of the first wall in a Helias reactor, which is roughly twice as large as in the equivalent tokamak reactor (fusion power 3000 MW), the initial installation of the breeding blanket requires nearly two times larger. However, since the neutron wall load is reduced, the lifetime of blanket components is roughly twice as long. Therefore, integrated over the lifetime of the fusion reactor (30 years), the amount of breeder material is nearly the same. This argument is also true for the amount of nuclear waste at shutdown of the power plant.

First steps are being made to develop an integrated concept of the stellarator power plant including the buildings and the thermal conversion cycle. This work is in progress, and it is envisaged to obtain rough cost estimates of a stellarator power plant.